

## Short Note

# Crustal Thickness Variations across the Blue Ridge Mountains, Southern Appalachians: An Alternative Procedure for Migrating Wide-Angle Reflection Data

by Robert B. Hawman

**Abstract** Migration of wide-angle reflections generated by quarry blasts suggests that crustal thickness increases from 38 km beneath the Carolina Terrane to 47–51 km along the southeastern flank of the Blue Ridge. The migration algorithm, developed for generating single-fold images from explosions and earthquakes recorded with isolated, short-aperture arrays, uses the localized slant stack as an intermediate data set. In contrast with other methods, it includes an interpretive step that is based on the assumption that all coherent *P*-wave energy consists of reflections from planar interfaces. Each sample in the slant stack is mapped into a planar, dipping segment with a length that is determined by the recording aperture. Migrated sections from within the Blue Ridge show increases in reflectivity at depths of 20 and 40 km. High apparent reflectivity from 40 to 50–55 km suggests a layered zone in the lower crust that is similar to models proposed for the Cumberland Plateau in Tennessee and the Adirondacks. The migration results are consistent with regional gravity data and with the occurrence of crustal roots beneath the Urals, another Paleozoic orogen.

### Introduction

The main objective of this study was to map variations in crustal thickness and seismic-wave velocity structure across the southwest end of the Blue Ridge province, southern Appalachians (Fig. 1) in order to test various models for isostatic compensation of mountain topography and high-density structures within the crust. The wide-angle experiments supplement existing common-midpoint (CMP) profiles (Cook *et al.*, 1979; Hatcher *et al.*, 1987) by taking advantage of elevated reflection coefficients near the critical angle. The strategy followed in the present study was to deploy small-aperture arrays over a wide range of source-receiver distances (5–200 km) to constrain crustal velocities while keeping receiver spacing small enough (200 m) to provide unaliased recordings of wide-angle reflections for migration.

### Migration Algorithm

The migration algorithm described here (introduced in Hawman [2004] and discussed in the present paper in greater detail) was developed for generating single-fold images from data recorded with isolated, short-aperture arrays. The algorithm is an extension of the method described by Hawman and Phinney (1992) for migrating travel-time picks in common-source gathers. Like the methods described by Phinney and Jurdy (1979) and Milkereit (1987), it uses the

localized slant stack of the source gather as an intermediate data set. Unlike those methods, however, it includes an interpretive step that is based on the assumption that all coherent *P*-wave energy consists of reflections from planar interfaces.

The method uses ray tracing to determine the position and dip of reflecting interfaces (Fig. 2). The ray parameter fixes the angle of incidence of the wavefront across the array. Each sample in a ray-parameter trace (where time corresponds to travel time to the center of the array) is downward continued until it intersects a ray traveling downward from the source that yields a combined two-way time that matches the observed time. Dip is determined from the ray parameters of the upgoing and downgoing rays (Hawman and Phinney, 1992).

Once the position of the reflector midpoint is determined, an interface is generated by assigning the value of that slant-stack sample to all subsurface points along a linear segment with the appropriate dip (Fig. 2c). This is the interpretive step that assumes reflection from a planar interface. A separate subsurface section is generated for each ray-parameter trace. Each trace in a given section is linearly interpolated over depth. The sections then are stacked to construct an image of reflectors as recorded for that shot gather. The ray-parameter increment used for the slant stack is chosen small enough to ensure a slight overlap of reflector

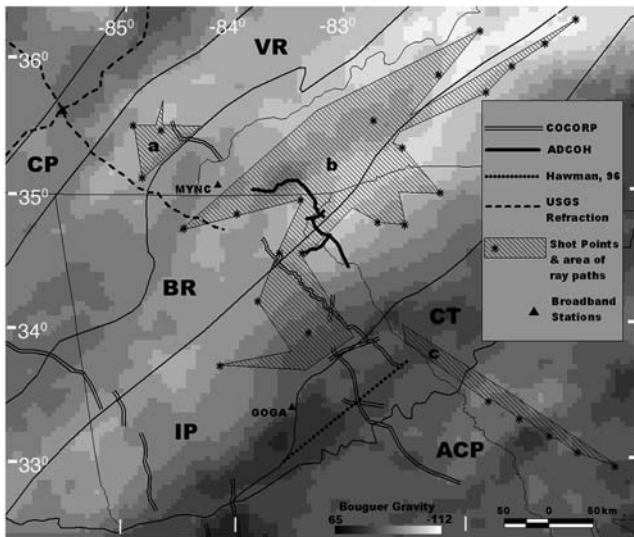


**Figure 1.** Bouguer gravity anomaly map of a portion of the southern Appalachians (after Baker, 2006; gravity data from Phillips *et al.*, 1993), showing the locations of seismic profiles. Labels are as follows: Cumberland Plateau, CP; Valley and Ridge, VR; Inner Piedmont, IP; Caroline Terrane, CT; Atlanta Coastal Plain, ACP. Double and heavy lines refer to Consortium for Continental Reflection Profiling (COCORP) (Cook *et al.*, 1979) and Appalachian ultra-deep corehole (Hatcher *et al.*, 1987) seismic reflection profiles, respectively. Dashed line in the northwest corner of the map is the refraction profile interpreted by Prodehl *et al.* (1984). Dotted line is the three-component, wide-angle profile of Hawman (1996). Hatching covers areas spanned by ray paths of three-component wide-angle recordings from (a) Hawman *et al.* (2001), (b) this study, and (c) R. Hawman (unpublished data, 1991). Triangles are USNSN broadband stations GOGA and MYNC.

segments for reflections spread out over several adjacent ray parameters. For the narrow recording apertures considered here (2–5 km), the effect of nonlinear move out of reflections is small, and smearing in the final image is due mostly to the finite beam width of the array.

For gentle dips, the portion of an interface actually sampled by a given shot will be roughly half the width of the array. This is the width used by the algorithm in generating linear segments for each sample in the slant stack. This approximation overestimates the reflector segment length actually sampled for reflections recorded downdip from the source and underestimates the segment length for reflections recorded updip. For the short arrays considered here, these effects are small compared with the smear in the image due to finite array beam width (Fig. 2d).

Reflections recorded updip from the source map into narrower smiles than reflections recorded downdip because of the convergence of upgoing ray paths as they approach the array. Stacking the sections for all ray parameters therefore tends to amplify updip reflectors because of the greater overlap of component segments. This can be remedied, at the expense of some additional smearing, by normalizing each sample in the final output section by its hit count.

Last, postcritical phase shifts will increase the phase velocity (decrease the ray parameter) of arrivals, causing errors in migrated dip. Again, for the small array apertures considered here, this shift in ray parameter is small compared with the array beam width.

Although the method is not a true wave-field migration, it does incorporate useful information from the input wave field into the migrated image. The dimensions of migration smiles are controlled by the degree of smearing in the slant stack, which in turn is controlled by the array aperture and signal bandwidth. The dimensions of these smiles thus serve as measures of the resolving power of the input gather.

### Comparison with Other Migration Methods

Phinney and Jurdy (1979) use slant stacks of common-source gathers from CMP profiles to back-project reflection energy into the subsurface. A complete image is formed by stacking results for individual gathers. Milkereit (1987) divides wide-angle profiles into overlapping, narrow-aperture spatial windows, then uses the semblance of the localized slant stacks of those windows to identify coherent arrivals in the  $T(x)$  domain for input into a diffraction-stack migration. In this approach, contributions to the migrated image are restricted to input samples that arrive with the travel times and ray parameters predicted for diffraction through a velocity model. This improves spatial resolution by suppressing contributions from coherent noise.

Both of the earlier approaches correctly handle diffractions. Structure is brought into focus by summing the contributions from many overlapping source-receiver pairs. In contrast, the algorithm described here uses the *a priori* assumption of specular reflection to generate planar reflection segments directly from isolated, small-aperture source gathers, without contributions from neighboring or overlapping spatial windows. In essence, we are cheating in an attempt to extract interpretable information from a very limited data set.

The migration smiles generated by the new algorithm are fundamentally different from those generated by true wave-field migration. In the new algorithm, each sample in the slant stack is mapped into a line that is tangent to the equal-time surface, while in conventional migration, each sample is mapped into an arc that follows this surface exactly (Fig. 2d).

Given a profile with multifold coverage, the more robust result produced by true wave-field migration will be preferred, but for single-fold coverage, especially recordings of explosions or earthquakes made with isolated, short-aperture arrays, the present method can be useful.

### Experiments in the Blue Ridge Mountains

The algorithm is being used to migrate a set of roughly 115 timed quarry blasts recorded along the East Coast gravity high (Carolina Terrane), the Appalachian gravity gradient (Inner Piedmont), and the Appalachian regional gravity low (Blue Ridge). The 50 blasts recorded in the Blue Ridge be-

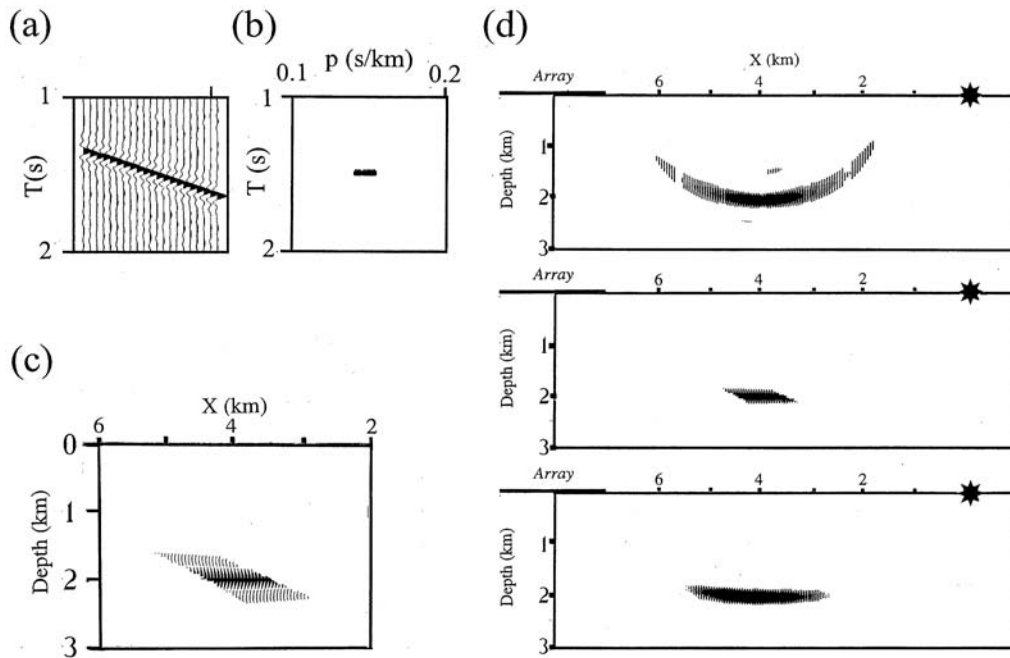


**Figure 2.** Migration of synthetic data. (a) Synthetic shot gather with one reflection (zero-phase wavelet) and white noise, generated for a layer of velocity 6 km/sec over a discontinuity (zero dip) at a depth of 2 km. Station spacing: 100 m; distance range: 7–9 km; trapezoidal passband for signal and noise: 2, 4, 15, 20 Hz. (b) Slant stack of the shot gather in (a), coherency filtered using the method of Kong *et al.* (1985). Vertical axis corresponds to travel time to the center of the array. (c) Migration of a single ray-parameter trace ( $p = 0.149$  sec/km), using the method described in the text. The wavelet is mapped into a trapezoidal region in the migrated section. The asymmetry of the trapezoid, with its wide end on the array side of the image, is the result of single-sided recording. (d) Comparison of migration output. Top: phase-shift migration (Gazdag, 1978) of the gather in (a) after application of normal move-out correction. Two-way normal time has been converted to depth. Middle: migration shown in (c). Bottom: migration of all ray-parameter traces in (b). Overlap of reflector segments generated by samples from adjacent ray-parameter traces generates amplitude fluctuations that vary laterally, but the overall shape preserves the dip.

tween 2002 and 2004 sample the highest elevations (2040 m) in the Appalachians. The experiments were carried out with a portable array of 20 digital seismic recorders (PRS-4) with three-component, 4.5-Hz geophones. Station spacings ranged from 50 to 250 m; source-receiver distances ranged from 6 to 200 km.

### Processing

All blasts in the Blue Ridge were ripple fired. Source durations ranged from 0.2 to 1.0 sec; most were less than 0.5 sec. For the work described here, deconvolution of shot gathers prior to migration was limited to spectral whitening. This was carried out using a zero-phase filter that normalizes the amplitude spectrum (Jurkevics and Wiggins, 1984). The algorithm was modified so that the normalization was applied only for frequencies with relative amplitudes above a specified threshold (between 0.01 and 0.1). The main purpose of whitening was to minimize variations in waveforms due to variations in site response for stations across a given array. The resulting increase in bandwidth also reduces ringing (Hawman, 2004), but the complete removal of the effects of ripple firing requires a filter operator that is not zero phase. A more thorough approach to deconvolution based on estimates of source wavelets is described in Hawman (2004).

Slant stacks were computed for a reference time corresponding to the mean offset of the array. The slant stacks were coherency filtered to isolate the most reliable events for migration. Coherency was evaluated by computing the semblance for a time gate of one sample; the semblance traces then were smoothed by high-cut filtering and a coherency filter implemented by setting to zero all samples in the corresponding slant stack with smoothed semblance below a specified threshold (Stoffa *et al.*, 1981). In choosing values for the threshold, it was assumed that noise in the record is stationary (Robinson and Treitel, 1980). The time window immediately preceding the first arrival was used to characterize the noise level for the entire record. The coherency threshold was raised until less than 1% of the samples in this noise window remained. It was found that a value of about 1% leaves waveforms of events in the signal windows largely intact (Fig. 3b). The threshold was raised further to minimize smearing of individual events along the ray-parameter axis (Fig. 3c). Events with amplitudes smaller than those of events remaining in the noise window were not included in the migration. Events interpreted as *P*-*SV* conversions and *S*-wave reflections that fall along roughly parallel trends at higher ray parameters (Fig. 3b) were also excluded.

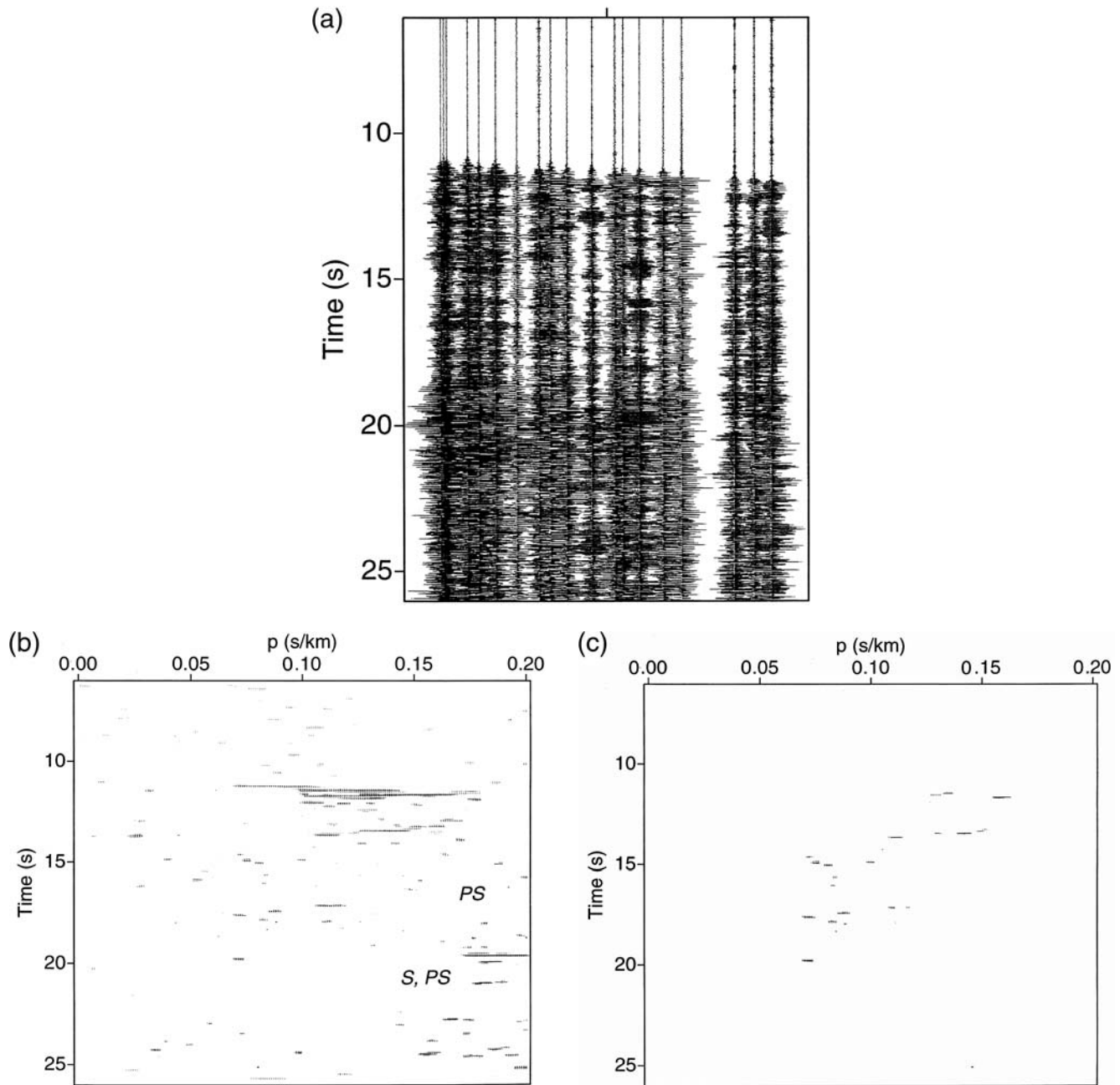


**Figure 3.** Sample data for a blast recorded along a north-south azimuth at distances of between 66.1 and 69.9 km. (a) Unfiltered shot gather. Direct  $P$  waves arrive at roughly 11–11.6 sec, and direct  $S$  waves arrive at roughly 19–20 sec. (b) Coherency-filtered slant stack of (a), after whitening and bandpass filtering (4–50 Hz). Time axis corresponds to the travel time to the center of the array. The threshold for the coherency filter was adjusted to remove 99% of the samples in the 4-sec noise window preceding the first arrival. For nondipping interfaces, the ray parameter for reflections will decrease with arrival time; dip introduces scatter about this trend.  $P$ - $SV$  conversions ( $PS$ ) and  $S$ -wave reflections ( $S$ ) occur in separate bands at higher ray parameters, in part beyond the range in ray parameter shown here. (c) Same as (b), but showing only those events used for migration (Fig. 4a). The coherency threshold has been raised for some events to reduce smearing along the  $p$  axis.

### Migration Results and Conclusions

Preliminary velocity models for the Blue Ridge derived from inversion (Zelt and Smith, 1992) of first arrivals and strong events interpreted as reflections from the Moho suggest an average crustal velocity of 6.5–6.6 km/sec and

a crustal thickness of 50–55 km. The average velocity is greater than the global average for continental crust (6.45 km/sec) reported by Christensen and Mooney (1995), but is close to the value (6.6 km/sec) found by Prodehl *et al.* (1984) for the crust in the western Blue Ridge and eastern Tennessee Valley and Ridge.

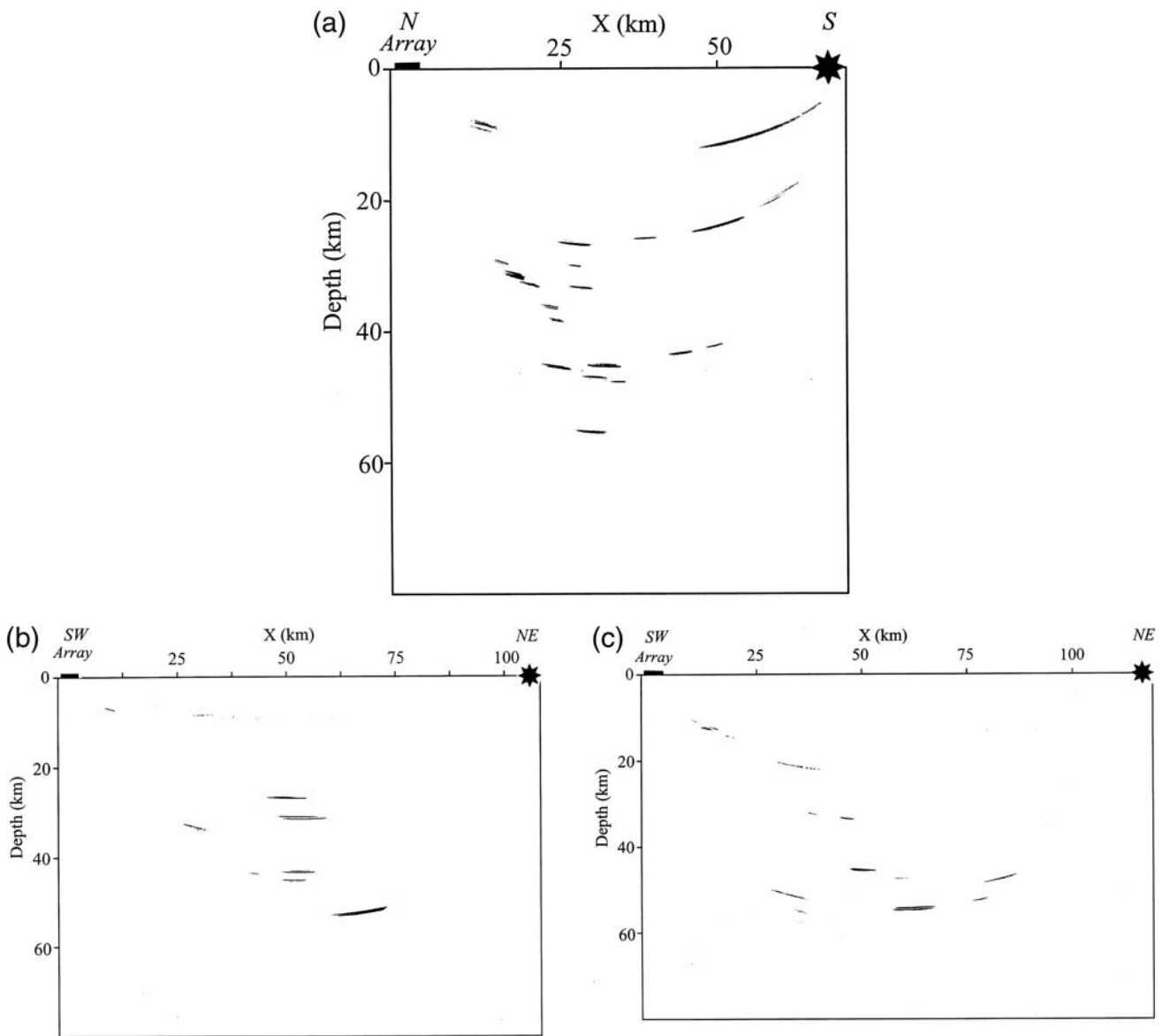


**Figure 4.** Representative migrated sections (no vertical exaggeration) across the Blue Ridge Mountains. Each section was generated from a single blast recorded with a short-aperture (2–5 km) array using the algorithm described in the text. Ray-parameter increment used for the slant stack: 0.0002 sec/km; sampling interval: 0.005 sec; spacing of output traces: 250 m; depth increment for output traces: 10 m. Deconvolution of shot gathers prior to migration was limited to spectral whitening. Source durations for most of the ripple-fired blasts were less than 0.5 sec (for the blasts shown: 0.26–0.34 sec). Possible overestimates of depth associated with migration of later cycles in the ripple-fired waveforms vary with incidence angle; for a 0.5-sec delay (corresponding to maximum amplitudes near the end of a 0.5-sec source wavelet), they range from 1.5–4 km. This type of error can be reduced by using minimum-entropy deconvolution to estimate and remove the ripple-fired wavelet (Hawman, 2004) prior to migration. (a) North–south ray paths with midpoints just inside the southeast flank of the Blue Ridge, near a local minimum in the regional Appalachian gravity low. Source duration: 0.34 sec. Note the clustering of reflectors at depths between 45 and 48 km, and the reflector (Moho?) at 55 km. (b) Southwest–northeast ray paths, with midpoints near the southeast flank of the Blue Ridge. Source duration: 0.29 sec. A strong reflector interpreted as the Moho appears at depths between 51 and 53 km. (c) Southwest–northeast ray paths with midpoints near the center of the Blue Ridge. Source duration: 0.26 sec. The strong reflectors at depths between 54 and 55 km are interpreted as Moho.

Migration of shot gathers (Figs. 4 and 5) for the shorter-duration blasts suggests that crustal thickness increases from about 38 km beneath the Carolina Terrane (Hawman, 1996; Khalifa, 2002) to 47–51 km along the southeastern flank of the Blue Ridge province in North and South Carolina. Ana-

lysis of receiver functions computed for United States National Seismic Network (USNSN) broadband stations GOGA (Carolina Terrane/Inner Piedmont boundary) and MYNC (Blue Ridge) shows a similar variation in crustal thickness (Baker and Hawman, 2006). Migrated sections

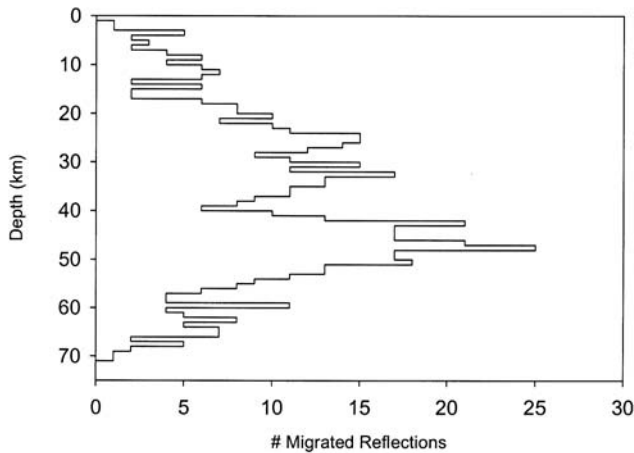


**Figure 5.** Distribution of migrated reflections as a function of depth for 36 quarry blasts recorded in the Blue Ridge Mountains, derived by summing the total number of migrated reflectors over 1-km bins. Shot-receiver distances for the field gathers ranged from 6 to 200 km. Reflections for migration were picked from coherency-filtered slant stacks, as explained in the text. Note the sharp increase in the number of migrated reflections at depths of roughly 20 and 40 km; the latter marks the top of a zone with high apparent reflectivity in the deep crust that extends to depths of 50–55 km. Note also the less pronounced peaks at roughly 60 km within the upper mantle.

from within the Blue Ridge show an increase in the number of reflectors at depths of roughly 20 and 40 km (Fig. 5). The latter depth marks the top of a zone with high apparent reflectivity in the deep crust that extends to depths of 50–55 km, suggesting the possibility of a layered zone that is similar to models proposed for the Cumberland Plateau of Tennessee (Owens *et al.*, 1984; Prodehl *et al.*, 1984) and the Adirondacks (Owens and Zandt, 1985). One factor contributing to the enhanced reflectivity could be the emplacement of mafic sills into less mafic crust, with reflection amplitudes boosted significantly by tuning effects (Costain *et al.*, 1989).

A gradual decrease in the number of reflectors between 50 and 55 km reflects variations in crustal thickness (Fig. 6). Crustal thickness within this portion of the Blue Ridge Mountains varies between 46 and 55 km, with a minimum value observed beneath the Asheville Basin (Fig. 6), suggesting that mountain topography may be supported by Airy-type crustal roots. Less pronounced peaks in the number of migrated reflectors occur at roughly 60 km (Fig. 5). These correlate with conversion depths in the uppermost mantle for events that arrive shortly after the  $P_s$  conversion from the Moho in receiver functions for USNSN station MYNC (Baker and Hawman, 2006). An apparent increase in reflectivity also occurs at 8 km, near the projected depth of the top of North American basement (Hatcher *et al.*, 1987; Hubbard *et al.*, 1991).

These findings differ significantly from previous models based on CMP data (Cook *et al.*, 1979; Hubbard *et al.*, 1991)

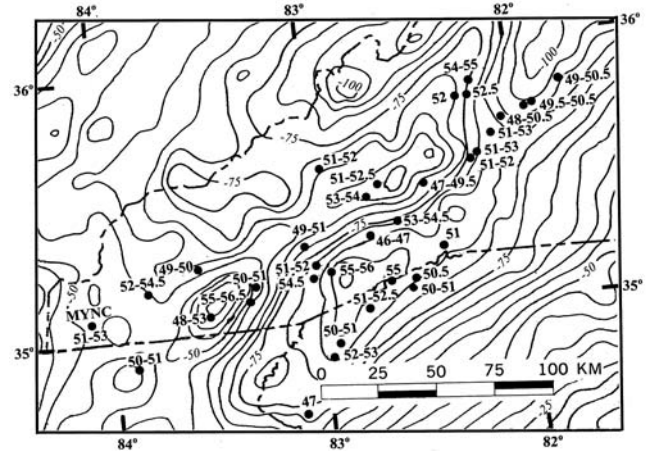


**Figure 6.** Crustal thickness for a portion of the southern Appalachians, determined from migration of events interpreted as wide-angle reflections from the Moho. Contours are Bouguer gravity anomalies (after Society of Exploration Geophysicists, 1982). Dots are ray path midpoints for individual blasts; thicknesses are in kilometers. Ranges in thickness for each midpoint incorporate the uncertainty in migrated depth due to finite signal bandwidth and aperture of the seismograph arrays. Average source/receiver elevations for individual recordings were  $680 \pm 360$  m. Crustal thickness increases from 38 km beneath the Carolina Terrane (Fig. 1) to 47–51 km beneath the foothills along the southeastern flank of the Blue Ridge province. Crustal thickness within the Blue Ridge Mountains varies from 46 to 55 km; the minimum thickness is found below the Asheville Basin.

that show a flat Moho dipping gently to a maximum depth of 43 km beneath the Blue Ridge. They are consistent, however, with regional gravity data (Hawman, 1996) and with the occurrence of crustal roots imaged by profiles crossing other Paleozoic orogens such as the Ural Mountains (Thouvenot *et al.*, 1995; Knapp *et al.*, 1998). The results suggest a way to more effectively utilize recordings of explosions and earthquakes made with small-aperture arrays. This type of recording can serve as a useful reconnaissance tool prior to the deployment of a large-scale experiment.

### Acknowledgments

The author thanks J. Clippard for technical assistance; S. Baker, C. Fortner, K. Gragg, P. Hawman, C. Jones, and B. Veal for their help with field work; and Feldspar Corporation, Hanson Aggregates, and Vulcan Materials for generous permission to monitor their blasts. In particular, the author thanks the following individuals for their assistance: A. Glover of Feldspar Corporation; R. Watkins, R. Crowe and M. Schwent of Hanson Aggregates; and J. Stroud, A. Shapiro, R. Allen, B. Allison, J. Brissey, C. Earnhardt, T. Hendrix, J. Marsh, C. Mash, L. Mims, S. Peek, W. Peek, W. Queen, T. Snapp, D. Verner, and J. Young of Vulcan Materials Company. The author also thanks B. Kloepfel, Coweeta Hydrologic Laboratory, K. Langdon, Great Smoky Mountains National Park, W. Carpenter and M. Wilkins, U. S. Forest Service, and personnel with the North Carolina and South Carolina Departments of Transportation for their help with logistics. A careful review by J. Costain improved the manuscript. This research was supported by National Science Foundation Grant Number EAR-0124249.

## References

- Baker, M. S. (2006). Investigation of the crust and uppermost mantle in the Carolina Terrane and Blue Ridge, southern Appalachians, using receiver function analysis of broadband earthquake data, *Master's Thesis*, University of Georgia, Athens, Georgia.
- Baker, M. S., and R. B. Hawman (2006). Combined wide-angle reflection and receiver function studies of the crust and upper mantle beneath the Carolina Terrane and Blue Ridge provinces, southern Appalachians, *Eighteenth Annual IRIS Workshop*, Tucson, Arizona, 8–10 June.
- Christensen, N. I., and W. D. Mooney (1995). Seismic velocity structure and composition of the continental crust: a global view, *J. Geophys. Res.* **100**, 9761–9788.
- Cook, F. A., D. S. Albaugh, L. D. Brown, S. Kaufman, J. E. Oliver, and R. D. Hatcher Jr. (1979). Thin-skinned tectonics in the crystalline southern Appalachians: COCORP seismic reflection profiling of the Blue Ridge and Piedmont, *Geology* **7**, 563–567.
- Costain, J. K., R. D. Hatcher Jr., C. Coruh, T. L. Pratt, S. R. Taylor, J. J. Litehiser, and I. Zietz (1989). Geophysical characteristics of continental crust, in *The Appalachian–Ouachita Orogen in the United States: The Geology of North America*, R. D. Hatcher Jr., W. A. Thomas and G. W. Viele (Editors), Vol. F-2, Geological Society of America, Boulder, Colorado, 385–416.
- Gazdag, J. (1978). Wave-equation migration by phase shift, *Geophysics* **43**, 1342–1351.
- Hatcher, R. D., Jr., J. K. Costain, C. Coruh, R. A. Phinney, and R. T. Williams (1987). Tectonic implications of new Appalachian ultradeep core hole (ADCOH) seismic reflection data from the crystalline southern Appalachians, *Geophys. J. R. Astr. Soc.* **89**, 157–162.
- Hawman, R. B. (1996). Wide-angle, three-component seismic reflection profiling of the crust beneath the East Coast gravity high, southern Appalachians, using quarry blasts, *J. Geophys. Res.* **101**, 13,933–13,945.
- Hawman, R. B. (2004). Using delay-fired quarry blasts to image the crust: A comparison of methods for deconvolving mixed-delay source wavelets, *Bull. Seismol. Soc. Am.* **94**, 1476–1491.
- Hawman, R. B., and R. A. Phinney (1992). Structure of the crust and upper mantle beneath the Great Valley and Allegheny Plateau of eastern Pennsylvania, part 2: Gravity modeling and migration of wide-angle reflection data, *J. Geophys. Res.* **97**, 393–415.
- Hawman, R. B., M. C. Chapman, C. A. Powell, J. E. Clippard, and H. O. Ahmed (2001). Wide-angle reflection profiling with quarry blasts in the East Tennessee seismic zone, *Seism. Res. Lett.* **72**, 108–122.
- Hubbard, S. S., C. Coruh, and J. K. Costain (1991). Paleozoic and Grenvillian structures in the southern Appalachians: extended interpretation of seismic reflection data, *Tectonics* **10**, 141–170.
- Jurkevics, A., and R. Wiggins (1984). A critique of seismic deconvolution methods, *Geophysics* **49**, 2109–2116.
- Khalifa, M. O. (2002). Wide-angle seismic reflection studies of the Elberton granite and Carolina Terrane, southern Appalachians, northeast Georgia, *Ph.D. Thesis*, University of Georgia, Athens, Georgia.
- Knapp, J. H., C. C. Diaconescu, M. A. Bader, V. B. Sokolov, S. N. Kashubin, and A. V. Rybalka (1998). Seismic reflection fabrics of continental collision and post-orogenic extension in the Middle Urals, central Russia, *Tectonophysics* **288**, 115–126.
- Kong, S. M., R. A. Phinney, and K. Roy-Chowdhury (1985). A nonlinear signal detector for enhancement of noisy seismic record sections, *Geophysics* **50**, 539–550.
- Milkereit, B. (1987). Migration of noisy crustal seismic data, *J. Geophys. Res.* **92**, 7916–7930.
- Owens, T. J., and G. Zandt (1985). The response of the continental crust-mantle boundary observed on broadband teleseismic receiver functions, *Geophys. Res. Lett.* **12**, 705–708.
- Owens, T. J., G. Zandt, and S. R. Taylor (1984). Seismic evidence for an ancient rift beneath the Cumberland Plateau, Tennessee: a detailed analysis of broadband teleseismic P waveforms, *J. Geophys. Res.* **89**, 7783–7795.
- Phillips, J. D., J. S. Duval, and R. A. Ambroziak (1993). National geophysical data grids: gamma-ray, gravity, magnetic, and topographic data for the conterminous United States, in U.S. Geol. Surv. Digital Data Series Map DDS-9, Denver, Colorado. Available on CD-Rom.
- Phinney, R. A., and D. M. Jurdy (1979). Seismic imaging of deep crust, *Geophysics* **44**, 1637–1660.
- Prodehl, C., J. Schlittenhardt, and S. W. Stewart (1984). Crustal structure of the Appalachian highlands in Tennessee, *Tectonophysics* **109**, 61–76.
- Robinson, E. A., and S. Treitel (1980). *Geophysical Signal Analysis*, Prentice Hall, New York, 466 pp.
- Society of Exploration Geophysicists (SEG) (1982). Gravity anomaly map of the United States, Tulsa, Oklahoma.
- Stoffa, P. L., P. Buhl, J. B. Diebold, and F. Wenzel (1981). Direct mapping of seismic data to the domain of intercept time and ray parameter: a plane wave decomposition, *Geophysics* **46**, 255–267.
- Thouvenot, F., S. N. Kashubin, G. Poupinet, V. V. Makovskiy, T. V. Kashubina, P. Matte, and L. Jenatton (1995). The root of the Urals: evidence from wide-angle reflection seismics, *Tectonophysics* **250**, 1–13.
- Zelt, C. A., and R. B. Smith (1992). Seismic traveltimes inversion for 2-D crustal velocity structure, *Geophys. J. Int.* **108**, 16–34.

Department of Geology  
University of Georgia  
Athens, Georgia 30602

Manuscript received 13 January 2007